Publications of the Astronomical Society of the Pacific, **118**: 1550–1557, 2006 November

POETS: Portable Occultation, Eclipse, and Transit System

Steven P. Souza,[1] Bryce A. Babcock,[2] and Jay M. Pasachoff[1]

Hopkins Observatory, Williams College, 33 Lab Campus Drive, Williamstown, MA 01267-2565; ssouza@williams.edu, bbabcock@williams.edu, jmp@williams.edu

Amanda A. S. Gulbis, J. L. Elliot,[3,4] and Michael J. Person

Department of Earth, Atmospheric, and Planetary Sciences, Massachusetts Institute of Technology, 77 Massachusetts Avenue, Cambridge, MA 02139-4307; gulbis@mit.edu, jle@mit.edu, mjperson@mit.edu

and

Joseph W. Gangestad[5]

School of Aeronautics and Astronautics, Purdue University, 315 North Grant Street, West Lafayette, IN 47907-2023; jgangestad@gmail.com

Received 2006 September 14; accepted 2006 September 25; published 2006 November 16

ABSTRACT. Occultations of stars by small bodies in the outer solar system are opportunities to make high-resolution measurements of their geometries and orbital elements and to detect or probe their atmospheres. Such events are limited in space and time, so it is desirable to deploy highly capable camera systems on multiple fixed and/or portable telescopes anywhere in the world, potentially on short notice. Similar considerations apply to planetary transits and solar eclipses. We have designed a camera system called POETS (Portable Occultation, Eclipse, and Transit System), which is optimized for occultation and related observations, and have assembled five such systems. The core of this system is the Andor Technology DV-887 (now DU-897) frame-transfer camera, featuring a high frame rate, minimal dead time, high quantum efficiency, and low read noise. An electron-multiplying mode lowers effective read noise to below 1 e^- pixel^{-1} and is capable of photon counting. Each POETS includes a compact GPS timing system with microsecond accuracy, and a high-performance computer system capable of sustained fast frame rates. Each POETS is designed to be transportable as carry-on luggage and is adaptable to a wide variety of sites. POETS were deployed for the first time for the 2005 July 11 Charon occultation event, and they performed extremely well on telescopes with apertures from 0.6 to 6.5 m. Three POETS were subsequently deployed for the 2006 March 29 total solar eclipse, and five for the 2006 June 12 Pluto occultation.

1. REQUIREMENTS FOR OCCULTATION CAMERA SYSTEMS

Stellar occultations by planetary satellites and small solar system bodies, which according to the 2006 IAU resolution 5A include asteroids and Kuiper Belt objects (KBOs), are opportunities to make high-resolution observations of their physical and orbital properties, including any atmospheres that may be present. In an occultation, the combined orbital motions of the solar system body and the Earth cause the body to briefly occult the star as viewed from certain locations on the Earth. The event may last from a few seconds to a few minutes. Since the apparent angular size of the star is small with respect to the solar system body, the occultation is usually total, although refraction and scattering in an atmosphere may prevent the star's light from being completely excluded from the detected signal.

An occultation observation consists of time-series photometry of the combined light of the occulting and occulted objects, resulting in a light curve from which information is extracted (Elliot & Olkin 1996; Elliot et al. 2003a). The photometric instrument of choice in the 21st century for visible and near-IR occultation observations is the CCD (charge-coupled device) camera. The velocity of the shadow of the solar system body, cast by the star as it passes across the Earth, is well known from orbital calculations (Olkin et al. 1996; Smart 1977). The spatial resolution with which the body is probed is therefore excellent, limited only by the small angular diameter of the star, Fresnel diffraction, and the time resolution of the observations. For example, during the 2002 August 21 occul-

[1] Department of Astronomy, Williams College, 33 Lab Campus Drive, Williamstown, MA 01267-2565.

[2] Department of Physics, Williams College, 33 Lab Campus Drive, Williamstown, MA 01267-2565.

[3] Department of Physics, Massachusetts Institute of Technology, 77 Massachusetts Avenue, Cambridge, MA 02139-4307.

[4] Lowell Observatory, 1400 West Mars Hill Road, Flagstaff, AZ 86001.

[5] Hopkins Observatory, Williams College, 33 Lab Campus Drive, Williamstown, MA 01267-2565.

tation of P131.1 by Pluto (Elliot et al. 2003b; Pasachoff et al. 2005), the shadow velocity at the Mauna Kea Observatory 2.2 m telescope was about 6.8 km s^{-1}, and the time resolution was 0.5 s, resulting in a maximum spatial resolution of about 3.4 km. An occultation camera system should thus be capable of a fast cadence; that is, intervals between exposure time centers of at least 0.1 s, preferably 0.01 s or faster. Slower cadences must also be supported to allow for higher signal-to-noise ratios (S/Ns) in the cases of fainter stars (likely for KBOs) or slower shadow velocities.

For these events, the occulted star is often only moderately bright ($m_R \approx 11$–15) and the available telescopes are modest in aperture (0.35–1.0 m). Including the light from the occulting body (which may dominate), and at the coarsest useful time resolutions of about a second, there is rarely a surplus of light, so it is imperative that nearly all photons arriving at the camera be recorded. The photometric camera system should therefore have (1) high QE (quantum efficiency), (2) a high filling factor (little light lost due to pixel geometry), (3) a high duty cycle (dead time between frames is much less than the exposure time), and (4) very low read noise, so detected photons are not obscured (masked) prior to digitization.

The shadow of the occulting object, cast in nearly parallel light from the distant star and thus appearing at the same size as the object, sweeps rapidly across a small fraction of the Earth's surface, typically only part of that being over land (Fig. 1).[6] This path may or may not include fixed-site telescopes of sufficient aperture. The uncertainty in the location of the shadow path is of the order of the occulting object's radius, and predictions of the shadow path location may be revised up until days before the event. As a result, a primary requirement for an occultation camera system is a high degree of portability. We define high portability as the ability to deploy the system to any fixed telescope site in two carry-on luggage items, one for each member of an observing team of two, on commercial air transportation. Specifically, airfreight should be avoided, because of possibly long shipping and customs delays, which are incompatible with last-minute changes in destination, and transportation as checked luggage should be avoided whenever possible, because of concerns over damage, loss, delays, and unpredictable restrictions by air carriers. At this time, most air carriers permit carry-on items with maximum dimensions of 9 × 14 × 22 inches (23 × 36 × 56 cm).

Another element of portability is the ability to operate on whatever AC power is available at the site, so we require universal (110–240 V AC) power supplies for all electronic components. The mechanical interface between the camera and the telescope should also be an industry standard (such as C-mount or T-mount) so that the system can be easily and quickly mounted on a wide variety of telescopes using commercially available or easily fabricated adapters.

[6] See http://occult.mit.edu/research/occultations/Charon/C313.2.html.

FIG. 1.—Predicted path of Charon's shadow during the 2005 July 11 occultation event. The outer lines indicate the predicted centerline and approximate width of the shadow's path across the Earth. The shading represents the portion of the Earth in darkness at the time of the event.

The system should be easily duplicated and straightforward to operate so that multiple teams can be fielded for an event. Even if the shadow path were perfectly known, multiple sites distributed perpendicular to the centerline of the shadow path are needed to accurately determine the size and geometry of an object. Uncertainties in the predicted path and weather conditions also argue for multiple sites.

An adjunct to high time resolution is high time accuracy. It is essential that the beginning and ending absolute UTC (Coordinated Universal Time) of each exposure be known to an accuracy much smaller than the cadence, to avoid geometry errors. It is desirable that those times be set up to the same accuracy well before the event; this correlation is especially useful when teams at multiple stations observe the same event. Another consideration related to high time resolution is the ability of the host computer to sustain the high data rate from the camera.

As this observation is fundamentally a photometric application, the camera must be highly linear, have minimal dead time between integrations, and have a moderately high dynamic range. Unlike many astronomical applications, there is no need for a very large field of view, and so a small CCD chip is acceptable. Although our focus is on occultation observations, most of these requirements also apply to observations of solar eclipses and planetary transits. The last includes a Venus transit in 2012 and transits of Mercury in 2006 and 2016.

Previous camera systems designed for occultation observa-

tions have been described elsewhere (Veverka et al. 1974; Elliot et al. 1975; Baron et al. 1983; Buie et al. 1993; Dunham 1995).

2. THE CAMERA

The full-frame (FF) CCDs predominant in astronomy can have an ~100% filling factor, QE peaking at over 90% (if back-illuminated), and excellent linearity and dynamic range. However, they cannot be read out fast enough to have a near 100% duty cycle for cadences at which we wish to operate. Interline-transfer (IT) CCDs are capable of high frame rates and are widely used in video applications (Howell 2006), but they generally have lower QEs and much lower filling factors than FF CCDs. IT CCDs usually include antiblooming gates to prevent overexposed regions of the chip from bleeding into other parts of the image. While essential for terrestrial video applications and useful in recreational astronomy, the intentional nonlinearity of antiblooming gates reduces photometric accuracy (AAVSO 2005 CCD Observing Manual, p. 8).[7] In addition, some manufacturers use a "microlens" over each pixel to collect light that would not otherwise reach the active area of that pixel, but the microlenses distort the point-spread function (PSF) of the chip (Pham et al. 2005), further compromising photometric accuracy.

Frame-transfer (FT) CCDs offer the best of both worlds and are the instruments of choice for faint-object occultation work. A FT CCD is essentially a FF CCD with an extra storage array adjacent to the imaging array (Howell 2006). The storage array is covered so that incoming light does not reach it. Clocking is arranged so that after an exposure is complete, the imaging array can be shifted into the storage array very quickly (a few ms) and then read out while the next exposure is under way. In this way, the readout process does not add to the interval between exposure centers, as long as the readout takes less time than the exposure itself. The resulting CCD has very high effective QE, linearity, and dynamic range. Its speed is intermediate between that of FF and IT types.

The operation of a FT CCD creates a unique artifact. FT CCDs (like IT, but unlike FF) are usually operated without a mechanical shutter, which would counteract much of their speed advantage. During the shift into the storage array, a bright point in the real image remains incident on the chip, potentially registering counts along a trail within the frame. For example, if the dwell time at each row during the shift is 5 μs and frames are taken at a rate of two per second (~500 ms exposure), light is deposited along the whole column at a level of 10^{-5} of the desired image. This effect is often negligible, but users of FT CCDs must be aware of it.

The noise in each pixel in each frame is largely determined by photon statistics, dark current, and noise contributed by the readout process. In modern CCD cameras cooled to -70°C or below, the dark current is generally insignificant and is not a factor for common exposure times in occultation observations. A trade-off is made between time resolution and S/N. One can increase the S/N by lengthening the exposure time at the expense of time resolution, and vice versa. It might seem that if a camera has a very high duty cycle it would always be advantageous to take data at the highest possible frame rate and then add every N adjacent frames to achieve the best compromise between time resolution and S/N. This procedure works up to a point, but each of the many averaged frames contributes its read noise, while a single frame exposed for a longer time includes only one read-noise contribution. If the read noise is significant compared to the photon noise of a single frame, then adding N frames yields a lower S/N than taking a single frame with N times the exposure time.

The read noise of a CCD camera is fundamentally limited by noise contributed in the read channel on the chip itself. It is also dependent on the rate at which the CCD is read out; on an excellent device, the chip's contribution may be on the order of 3–5 e^- at a low readout rate of 20,000 samples s^{-1} (e2v Technologies 2003 CCD77 specification sheet), and higher at faster readout rates. Amplifier and analog-to-digital conversion stages, required to turn a CCD device into a camera, typically increase the read noise by a few e^-.

One approach to the exposure time trade-off is to make an exposure such that read noise is dominated by the photon noise of the source. In the case of an occultation, this limit must be calculated from the combined light of the star and the occulting object. At this operating point, frames may be combined after the fact without significant S/N penalty, since the source photon noise depends only on the number of photons detected and not the number of frames that have been added (Mackay et al. 2004).

Seen this way, the advantage of having the lowest possible read noise is that one can acquire more frames during an event without an S/N penalty, and can be flexible in data reduction and analysis. Two CCD chip manufacturers, e2v and Texas Instruments, currently make FT CCDs with an extra read-channel register incorporating electron multiplication. The resulting gain, although not noiseless, occurs before other noise contributions from analog gain and digitization in the camera electronics. This multiplication can make the effective read noise less than 1 e^-, allowing photon noise to dominate even at very low photon rates. One FT CCD device that incorporates this feature is the e2v CCD97 sensor. With subelectron read noise and very high frame rates (e2v Technologies 2003 CCD97 specification sheet), it can even be operated in a photon-counting mode (Basden et al. 2003; Tulloch 2004).

Ideally, no aspect of the camera should compromise the limits set by the chip, but this condition is not guaranteed. Analog and digital electronics, cooling capacity and regulation, weight, size, calibration, mechanical mounting, hardware interface, software, and vacuum chamber design all contribute to the performance and usability of the system. The vacuum chamber

[7] The observing manual is available online: http://www.aavso.org/observing/programs/ccd/manual.

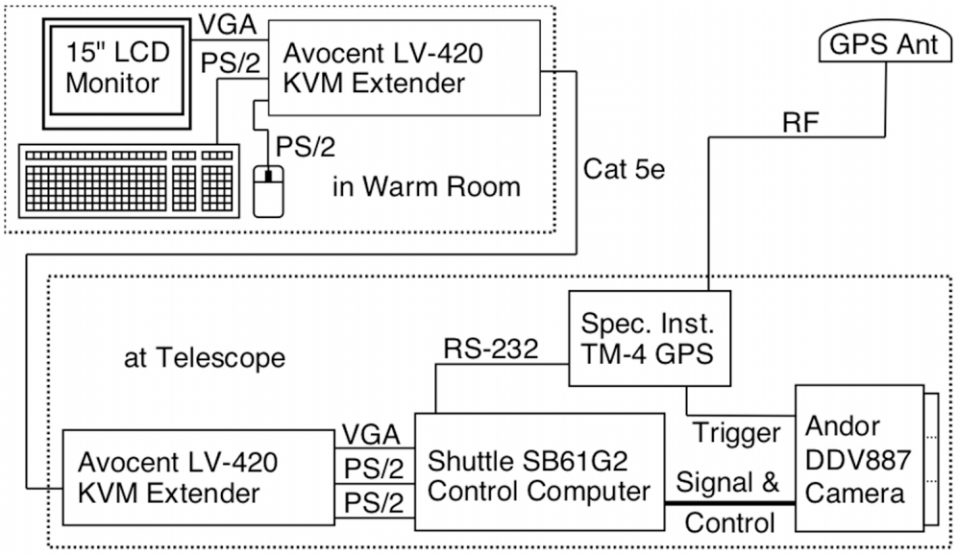

FIG. 2.—Block diagram of the POETS setup. POETS is designed to be used at an observatory with a warm room isolated from the telescope dome, so the user interface is deployed remotely from the control computer with a KVM extender. At smaller telescopes, this can be eliminated, and the keyboard, mouse, and monitor can be attached directly to the control computer.

is of particular interest. CCD cameras incorporate a clear window between the chip and the exterior of the camera, and the space between the chip and the window is either evacuated or filled with inert gas. This chamber both protects the chip and, by insulating the window from the cold parts of the camera, reduces the chance of condensation when the chip is cooled. If the vacuum space is not hermetically sealed, measures to ensure a dry environment in front of the window, such as a flow of dry nitrogen, may be needed. A permanent vacuum chamber that does not require periodic pumping is highly desirable.

The commercially available camera that we have chosen is Andor's iXon DV-887-BI (now DU-897). This FT camera has 16 μm square pixels in a 512 × 512 format. Its read noise and full-frame readout rate range from 6 e^- pixel^{-1} and 3 Hz in conventional mode to less than 1 e^- pixel^{-1} and greater than 30 Hz in electron-multiplying (EM) mode. Faster readout rates can be achieved by binning or reading out only a portion of the full frame. Operation in conventional mode at a 1 MHz readout rate provides 16 bit digitization, while all other operating modes provide 14 bit data. The camera meets the above requirements, weighs about 3.3 kg in a sufficiently compact form, and is delivered with Windows-based acquisition, control, and image-processing software that provides the user sufficient functionality for occultation observations.

3. SYSTEM DESIGN

Although the camera is the critical component in meeting the bulk of our performance goals, system design determines the overall suitability of the system for occultation observations. Figure 2 presents a block diagram of POETS. The system can be deployed to nearly any observatory (we have used it on telescopes ranging from 0.6 to 6.5 m). The only item that is not predetermined is the physical interface to the telescope, which we fabricate as needed. We emphasize that the entire system must fit in two airline carry-on cases; for this we chose a Lightware case, model MF2012, as it has the most interior room (7 × 11 × 20 inches; 18 × 28 × 51 cm) of any airline-compliant carry-on, and it offers considerable protection.

3.1. Control Computer

Camera selection places constraints on the control computer. We had expected to use a laptop computer for its portability but found that the hardware interface and hard disk performance requirements could only be met with a desktop system. High-throughput cameras require a dedicated interface that is proprietary to the camera manufacturer. Standard interfaces, such as FireWire and USB2.0, while featuring high peak data rates, do not support the sustained data rates of these cameras, nor do they permit full camera control and real-time control response. The Andor interface is a full-height PCI card, 200 mm in length.

While the laptop PCI problem might have been overcome, laptops compromise performance factors that are important for fast image acquisition, notably disk speed. High image acquisition rates require a fast processor, a very fast hard disk, and a large amount of system memory. At the recommendation of the camera manufacturer, we specified a ≥3.0 GHz Pentium 4 class processor, 2 Gbytes of main memory, and a 10,000 rpm hard disk. Disks of this speed are only available with SCSI

and Serial-ATA (SATA) interfaces; but while SCSI disks are no longer found on consumer computer systems, SATA is becoming ubiquitous. We also require a DVD-RW drive to make backup copies of our data in the field.

We therefore specified a desktop PC with the performance listed above, a PCI slot with room to accommodate a 200 mm long full-height PCI card, and dimensions no greater than approximately 7 × 8 × 11 inches (18 × 20 × 28 cm) to fit in a carry-on suitcase. In recent years, Windows-based computers known as "small form factor" (SFF) PCs have emerged, principally for the computer gaming market. Many such models satisfied our requirements in all ways except one, usually the accommodation of the Andor PCI card or the maximum 7 inch dimension. We therefore chose the Shuttle SB61G2 computer, one of the few that met all our requirements. The remaining PC-related components (keyboard, mouse, etc.) were dictated mainly by packing constraints. In particular, we chose the 15 inch Sony SDM-S53/B LCD monitor as the largest display that would fit in the carry-on case, although displays are often available at the target sites.

3.2. Timing

The next critical system component is a means of accurately timing the observations. Traditional methods of timing, such as WWV radio signals, have been made obsolete by the Global Positioning System (GPS), which inherently incorporates timing signals that are far more accurate than needed for occultation work. In the past, GPS timing could be derived using either very expensive systems designed for the TV broadcast industry, or by designing and building one's own system. The rapid fall in price of consumer handheld portable GPS systems makes it tempting to use these, but since they are designed primarily for navigation, their timing accuracy is generally on the order of 1 s, which is inadequate for this work. Some consumer GPS systems also provide an accurate pulse output at 1 s boundaries, but the UTC times of these pulses are not labeled, and other intervals cannot be set. In the future, the European Galileo system may provide added time resolution.

We have chosen the TM-4 GPS timing system from Spectrum Instruments, Inc. The TM-4 requires a small antenna to be deployed outside the dome. This system provides flexible timing that is accurate to well under 1 μs with respect to absolute UTC, and it can be used in two modes. An input port can be used to record the times of externally triggered events, for example shutter openings from the camera. In this mode, triggering is done by the control computer, and one determines the beginning and ending times of individual exposures ex post facto. Alternatively, the TM-4 can be programmed to begin emitting a series of transistor-transistor logic (TTL) pulses of a chosen width and interval at a specified UTC. In this case, the camera is set to accept external triggers and waits in an enabled state for the pulse train from the GPS to begin. An advantage of this mode is that acquisitions can be set on precise UTC boundaries, possibly common among several sites, to simplify later data analysis.

3.3. Remote Operation

At a small telescope, the operator's workstation can be located along with the control computer within the dome and connected to the camera with a 6 m cable supplied by the camera vendor. At a large telescope, however, a preferable arrangement is to have the monitor, keyboard, and mouse located in a warm room while the control computer rides with the camera or otherwise remains close to it. Long cables for video, etc., are problematic for signal quality and logistics, but devices known as "KVM extenders" (keyboard, video, mouse) allow the workstation components to be located remotely via a single Category-5e, unshielded, twisted-pair cable commonly used for Ethernet networks. We chose the Avocent LV-420 KVM extender, consisting of a transmitter box located with the computer and a receiver box located with the monitor, keyboard, and mouse. In our tests, this system provided more-than-adequate video quality and responsiveness with the computer and workstation separated by 200 feet of cable, although the KVM extender is specified for up to 500 feet, which is more than enough for any observatory. The LV-420 extender is the only POETS subsystem that was not supplied with universal power supplies by the vendor, so they were replaced with generic 110–240 V AC supplies.

Figure 3 shows the POETS system packed into two carry-on cases. Figure 4 shows the POETS cameras installed on a 0.6 m telescope at Observatório Pico Dos Dias in Brazil, and on a 6.5 m telescope of the Magellan project at Las Campanas in Chile. During operation, the camera is set up for an image sequence using Andor's software and is left waiting for a series of pulses from the GPS timing system. The GPS is set up to begin sending pulses at a specified UTC, at time intervals equal to the desired cadence. When the selected UTC is reached, the image sequence begins without user intervention. Typical parameters for the camera are kinetic acquisition mode, external triggering with positive polarity, series length of 12,000 frames, 16 bit readout at 1 MHz, 2 × 2 binning, and a gain of 0.7 e^- ADU^{-1} (analog-to-digital unit). Typical parameters for the GPS are multiple programmed output pulse mode with positive polarity, pulse width of 1 μs, pulse interval of 200 ms, and UTC of the first pulse 20 minutes prior to event center.

4. PERFORMANCE

During laboratory testing, the performance of the cameras was confirmed. Table 1 shows the gain and read noise for two cameras in conventional mode, and for one camera in EM mode. In all cases, the analog preamp gain was set to its maximum. Note that at low EM gain, the EM mode is highly disadvantageous, but at a nominal EM gain setting of 50, the read noise is driven below 1 e^-. The trade-off is reduced dynamic range; in this example, by a factor of roughly 2.

FIG. 3.—Photograph of a POETS unit packed in two airline-compliant carry-on cases.

The accuracy of the TM-4 timing system was tested against a computer system clock that was synchronized to UTC via NTP (Network Time Protocol) to better than 1 ms and was found to be accurate to within 1/60th of a second, the resolution of the accessible computer clock. In fact, we believe it to be far more accurate than this; the manufacturer specifies that pulse outputs are within 175 ns of specified UTC. For our purposes, it can be considered to be a "gold standard."

The first field test of POETS was during the 2005 July 11 occultation of a star designated C313.2 (=UCAC2 26257135; $m_R = 14.8$) by Charon, visible across a strip of South America (Fig. 1). The event was only the second stellar occultation by Charon ever to be observed, following an event 25 years earlier (Walker 1980), and the first to be observed from the multiple sites necessary for fitting a circular or elliptical profile and for finding Charon's diameter. The portability requirement was easily met, and deployment proved highly practical, with each carry-on case weighing no more than 14 kg. In the field, setup was fast and straightforward, and no significant problems were encountered on any of the four systems. Illustrating the flexibility of the system, POETS was used on 0.6 m (Fig. 4*a*) and 2.5 m equatorially mounted Cassegrain telescopes, a 6.5 m altitude/azimuth-mounted telescope at Nasmyth focus (Fig. 4*b*), and a 0.84 m equatorially mounted Newtonian telescope for this event. In all cases, the system performed to the telescopes' aperture and image quality limits, although clouds prevented observation on the 0.6 m telescope (Gulbis et al. 2006a). Figure 5 shows a single dark-subtracted frame from a 0.6 m telescope image sequence of the target field taken the night before the event. In this nominal 1 s exposure, the peak S/N of C313.2 is ~28, and the faintest stars that are reliably detected have an m_R of ~17.

Data are recorded as one or more multiple-image FITS files, along with bias frames and flat frames (twilight flats are used when possible, otherwise they are taken from a white target). At a chip temperature of −70°C and at the exposure times used in occultation work, there is no measurable difference between dark frames and bias frames. After optional subtraction of a mean bias frame and division by a mean flat, a light curve is produced via time-series photometry, which can be implemented as aperture photometry or using PSF-fitting methods (Stetson 1987). If aperture photometry is used, the additional step of mutually registering the frames can correct positional errors due to seeing and imperfect tracking and can increase

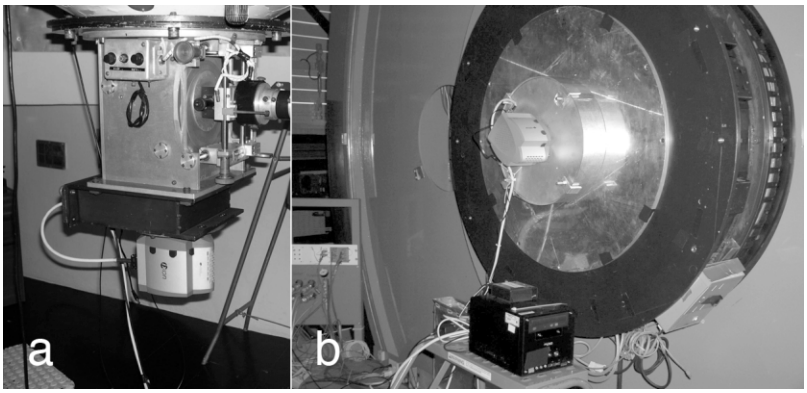

FIG. 4.—Photo of a POETS unit installed (*a*) on the 0.6 m telescope at Observatorio Pico Dos Dias, Brazil, and (*b*) at the Nasmyth focus of the 6.5 m Clay Telescope of the Magellan project at Las Campanas, Chile.

TABLE 1
MEASURED GAIN AND READ NOISE FOR TWO CAMERAS IN TWO MODES

Camera S/N	Mode	A/D (bits at MHz)	Gain (e^- ADU^{-1})	Read Noise (e^-)
X-1286	Conventional	16 at 1	0.70	5.2
X-2115	Conventional	16 at 1	0.68	5.6
	EM, gain = 1	14 at 10	13.5	56.2
	EM, gain = 50	14 at 10	0.15	0.67

the S/N of the final light curve by permitting use of a smaller aperture. We use IRAF,[8] ImageJ,[9] and our own routines, written in Mathematica, to perform this reduction. A representative light curve of the 2005 July 11 Charon occultation is shown in Figure 6. These data were taken on the du Pont 2.5 m telescope and have a S/N of 52 at full time resolution.

Our data consisted of three chords that enabled us to constrain Charon's radius to 606 km, ± 0.04 km statistical and ± 8 km allowing for topography and ellipticity (Gulbis et al. 2006a; Person et al. 2006). The result was improved accuracy in the radius, density, and rock-mass fraction of Charon. This in turn supports the idea that Charon was formed collisionally in the early solar system. Furthermore, the new value of Charon's radius can be used to fix one parameter in the solution of the mutual Pluto/Charon occultations (Binzel et al. 1985), giving an improved radius and density for Pluto itself. More recently, we deployed five POETS to Australia and New Zealand for the 2006 June 12 occultation of a star by Pluto, with similar success (Gulbis et al. 2006b; Elliot et al. 2006; Pasachoff et al. 2006a).

5. CONCLUSIONS

We have developed a portable camera system that is very well suited to high photometric and temporal quality observations of occultation events. The system is highly portable and adaptable to a wide variety of fixed-site and portable telescopes. Four such systems were deployed in South America for the 2005 July 11 Charon occultation event, and all were problem-free. Similar success was obtained in a deployment of five POETS to Australia and New Zealand for the 2006 June 12 Pluto occultation. Since many of the characteristics required of camera systems for solar eclipse and planetary transit events are similar to those for stellar occultations, we believe that these systems will perform similarly well in those applications; three were deployed in Greece for the 2006 March 29 total solar eclipse (Pasachoff et al. 2006b).

[8] See http://iraf.noao.edu.
[9] See http://rsb.info.nih.gov/ij.

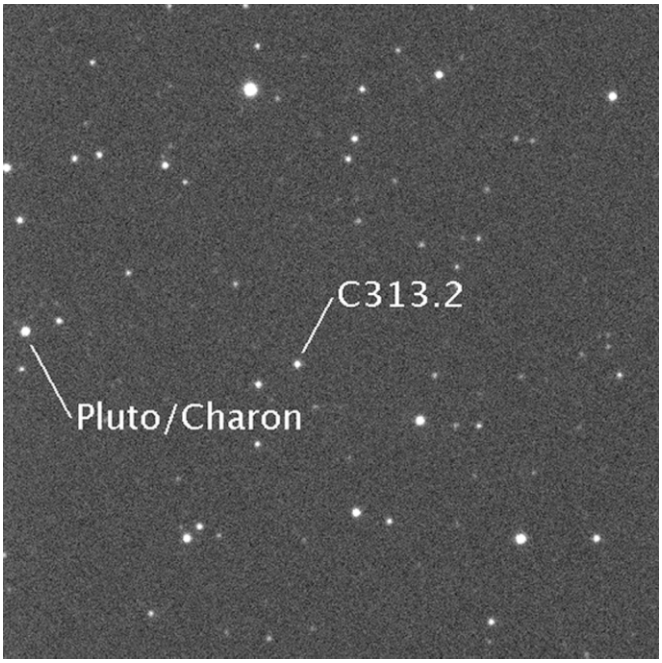

FIG. 5.—Single dark-subtracted frame from a sequence taken the night before the 2005 July 11 Charon event, obtained at the 0.6 m telescope at Pico Dos Dias, Brazil. The cadence was 1 frame s^{-1}, and the exposure time was 0.9982 s. Pluto/Charon and C313.2 are indicated; the m_R of C313.2 is 14.8.

Funding for this work has been provided by NASA Planetary Astronomy grants NNG 04GE48G (PI: J. L. E.), NNG 05GG75G, and NNG 04GF25G. We acknowledge the support of the Williams College Science Center.

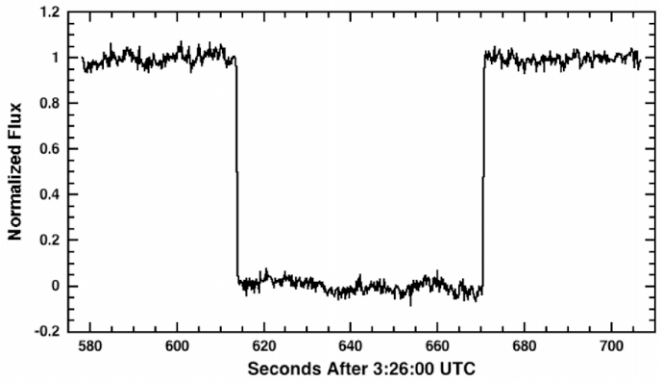

FIG. 6.—Light curve from the 2005 July 11 occultation of C313.2, obtained at the 2.5 m du Pont Telescope at Las Campanas, Chile. Fluxes have been normalized and shifted so that 1.0 represents the combined light of Pluto/Charon and C313.2, and zero represents the light of Pluto/Charon alone.

REFERENCES

Baron, R. L., Dunham, E. W., & Elliot, J. L. 1983, PASP, 95, 925
Basden, A. G., Haniff, C. A., & Mackay, C. D. 2003, MNRAS, 345, 985
Binzel, R. P., Tholen, D. J., Tedesco, E. F., Buratti, B. J., & Nelson, R. M. 1985, Science, 228, 1193
Buie, M. W., et al. 1993, BAAS, 25, 1115
Dunham, E. W. 1995, in ASP Conf. Ser. 73, Airborne Astronomy Symposium on the Galactic Ecosystem, ed. M. R. Haas, J. A. Davidson, & E. F. Erickson (San Francisco: ASP), 517
Elliot, J. L., & Olkin, C. B. 1996, Annu. Rev. Earth Planet. Sci., 24, 89
Elliot, J. L., Veverka, J., & Goguen, J. 1975, Icarus, 26, 387
Elliot, J. L., et al. 2003a, AJ, 126, 1041
———. 2003b, Nature, 424, 165
———. 2006, BAAS, 38, 31.02
Gulbis, A. A. S., et al. 2006a, Nature, 439, 48
———. 2006b, BAAS, 38, 31.01
Howell, S. B. 2006, Handbook of CCD Astronomy (2nd. ed.; Cambridge: Cambridge Univ. Press), 2006
Mackay, C. D., Baldwin, J., Lawn, N., & Warner, P. 2004, Proc. SPIE, 5492, 128
Olkin, C. B., Elliot, J. L., Bus, S. J., McDonald, S. W., & Dahn, C. C. 1996, PASP, 108, 202
Pasachoff, J. M., et al. 2005, AJ, 129, 1718
———. 2006a, BAAS, 38, 25.02
———. 2006b, BAAS, 37, 1.07
Person, M. J., Elliot, J. L., Gulbis, A. A. S., Pasachoff, J. M., Babcock, B. A., Souza, S. P., & Gangestad, J. 2006, AJ, 132, 1575
Pham, T. Q., van Vliet, L. J., & Schutte, K. 2005, Proc. SPIE, 5672, 169
Smart, W. M. 1977, Textbook on Spherical Astronomy (6th ed.; Cambridge: Cambridge Univ. Press)
Stetson, P. B. 1987, PASP, 99, 191
Tulloch, S. M. 2004, Proc. SPIE, 5492, 604
Veverka, J., et al. 1974, AJ, 79, 73
Walker, A. R. 1980, MNRAS, 192, 47